

D.5.1.1 One vulnerability and feasibility methodology for city, coastal and maritime area

Coordination group:
Università Iuav di Venezia

Main authors
Francesco Musco, Denis Maragno, Gianfranco Pozzer,
Filippo Magni, Giovanni Carraretto

Contributors
Matelda Reho, Giuseppe Piperata, Micol Roversi Monaco, Greta Masut

Contents

CONTENTS	2
1 INTRODUCTION	3
2 METHOD	5
2.1 Sources and data	6
2.2 Methods and data processing techniques	7
2.2.1 Landsat-8 imagery: analysis and processing data	8
2.2.1.1 Land surface temperature (LST)	11
2.2.1.2 Vegetation Health Index (VHI)	15
2.2.2 Using raster DTM for morphodynamic analysis	16
2.2.2.1 Surface runoff modelling	16
2.2.2.2 Areas Susceptible to Coastal Flooding due to SLR	18
2.2.3 Geoprocessing for spatial analysis	19
2.2.3.1 Geoprocessing applied to assessment of drought and wildfire	20
2.2.3.2 Geoprocessing applied to assessment of salt intrusion.....	22
2.3 Geodatabase	24
2.4 Vulnerability assessment methodologies: definition of assessment indicators	25
3 CONCLUSIONS	31
4 GLOSSARY	32
5 REFERENCES	33

1 Introduction

The work is part of the European Adriadapt Interreg Italy-Croatia programme coordinated by CMCC. The programme aims to improve the capacity of urban and coastal areas in the Adriatic area to respond to the effects of climate change.

The study analyses some types of impact potentially adverse to the dynamics of vulnerability of the following territories: Municipality of Udine; Municipality of Cervia; territories of Unione Valle Savio¹ (Emilia-Romagna); Municipality of Vodice (Croatia); Šibenik-Knin County (Croatia).

The analysis uses a selection of spatial databases appropriately cross-referenced, geo-referenced and elaborated in a multi-objective context: a database of cartographic material and documentary information (municipal, regional, national) on the status of infrastructure structures, settlement systems, morphologies and ecosystems.

This activity aims to develop a methodology for resilient representation of the territory and to provide local communities with efficient and effective climate change adaptation planning models. These models can ensure an adequate level of economic and social well-being for the local urban environment.

The work is divided into the following phases:

- collection of sources, data and information on knowledge, policy and planning frameworks, as well as on any pre-existing environmental vulnerability constraints;
- construction of a general interpretative model to support the definition of the selected impacts;
- guideline description of the areas of intervention, referred to available documentation;
- identification of the main impact relationships between the territorial characteristics and the environmental sectors considered;
- identification of the formulation of environmental vulnerability conditions;
- identification of strategic priorities for preventive adaptation to climate change, through a multi-disciplinary and multi-scale climate proof approach focused on local specificities.

¹ Municipalities of Bagno di Romagna, Cesena, Mercato Saraceno, Montiano, Sarsina, Verghereto.

The work will attempt to analyse and map the following impact dynamics:

- Urban Heat Islands
- Urban flooding/runoff
- Wildfire
- Drought
- Landslides
- Sea-level rise
- Salt intrusion

Impact	Udine	Cervia	Cesena (Comune dell'Unione Valle Savio)	Comuni dell'Unione Valle Savio	Vodice	Šibenik- Knin County ^[G1]
Urban Heat Islands	■	■	■		■	■
Urban flooding/runoff	■	■	■		■	■
Wildfire				■		■
Drought				■		■
Landslides				■		
Sea-level rise/coast erosion		■				■ ²
Salt intrusion		■				

Table 1 – Municipality/County and types of impact

² For the case of Šibenik-Knin County see the Coastal Plan (Margeta J. et al., 2016). The Coastal Plan is a best practice for sustainable coastal development. The Plan offers a series of recommendations and useful questions to define the first strategies for adaptation to climate change (both locally and regionally).

2 Method

The study proposes a methodology to assess the vulnerability of spatial morphologies and urban functions regarding the following impacts: high temperature; urban flooding (and landslides); wildfire (and drought); sea level rise; salt intrusion. The analysis has been conducted (with specific tests) in the territories of high Adriatic: Udine, Cervia, Cesena and Municipalities of the Savio Union (Italy); Vodice and Sibenik -Knin County(Croatia).

The vulnerability assessment is executed on a GIS environment in which impact and vulnerability are geographically specialized and visible in a set of maps. Using *ad hoc* statistical models (Maragno, 2018), it was possible to correlate the analysis of the impacts to geomorphological features by a variety of land use patterns and satellite indices.

This approach uses of a series of information and technological contents capable of quantifying the potential impacts through a rereading of the components of the vulnerability (figure 3, paragraph 2.4).

The proposed method allows application the first analytical assessments using a series of indicators classifiable by thematic orientation.

The impacts of climate change include multiple environmental interactions, which may in turn be related to other effects generated by climatic variations: variations caused by both exogenous and endogenous phenomena. The type of impact and its relationships with the sensitivity and adaptive capacity dimensions play a fundamental role in defining the vulnerability model, with significant differentiations respect to the relationship between the natural and anthropic areas of the territory (see paragraph 2.4).

The methodology includes four main stages:

1. Data source and data collection.
2. GIS techniques for the development of indices.
3. Construction of geodatabases.
4. Definition of guide models for vulnerability assessment.

2.1 Sources and data

This analysis uses a heterogeneous data basis for different application scenarios. The data refer to these two groups of spatial and alphanumeric information:

1. basic cartography for the urban and regional planning;
2. remote sensing data.

Category	Description	Format	Source	Processing
basic cartographic maps	<ul style="list-style-type: none"> • buildings, road networks, trees, rivers • digital terrain model (DTM) • SKC Coastal Plan maps collection 	Vector and raster	regional geographic information; open data	<ul style="list-style-type: none"> • definition of baselines • density ratios • modelling
thematic cartography	<ul style="list-style-type: none"> • land use • flood risk assessment and mapping (Direttiva Alluvioni 2007/60/CE) • costal plan • soil salinity map • landslide map landslide • map wildfire 	Vector and raster	regional geographic information systems; open data	<ul style="list-style-type: none"> • query e overlay analysis
remote sensing	satellite images	raster	Landsat 8 images (open data)	index: LST, NDVI, NDMI, TCI, VCI, VHI
meteorological data	thermo-pluviometric data	excel tables	web	<ul style="list-style-type: none"> • statistical analysis • monitoring and data evaluation

Table 2 – Territorial data collection: characteristics and elaborations

A specific database has been developed for each study area. The information content of each database is calibrated on the characteristics of the study area and its types of impact. These geodatabases used in a GIS-based multidisciplinary method, have provided the necessary evaluation elements to activate a technical-scientific analysis to support the definition of guidelines for adaptation to climate change.

2.2 Methods and data processing techniques

Data processing and GIS techniques allow the construction of SIT (System information territorial) for the evaluation of negative effects generated by extreme changes of climate. The analysis of impacts and vulnerabilities use a baseline methodology conducted with three data processing techniques:

1. processing of satellite images (Landsat-8);
2. processing of digital terrain models (DTM).
3. geoprocessing and spatial analysis.

Impact	Processing	Output
Urban Heat Islands	Elaboration of a synthetic index obtained from satellite images	<i>Land surface temperature (LST)</i>
Urban flooding/run off	Surface runoff modeling from DTM	<i>Surface runoff</i>
Wildfire	Elaboration of a synthetic index obtained from satellite images; GIS overlay analysis for the study of the spatial correlation between drought and wildfire	<i>Vegetation Health Index (VHI)</i>
Drought	Elaboration of a synthetic index obtained from satellite images; overlay analysis for the study of the spatial correlation between drought and wildfire	<i>Vegetation Health Index (VHI)</i>
Landslides	Overlay analysis for the study of the spatial correlation between runoff and landslides	<i>Surface runoff vs landslides</i>
Sea-level rise	Sea-level rise analysis from DTM	<i>Coastal flooding from sea-level rise</i>
Salt intrusion	Geoprocessing for the study the tolerance of tree species to soil salinity	<i>Soil salinity vs arboreal species</i>

Table3 – Data processing techniques used for the different types of impact

2.2.1 Landsat-8 imagery: analysis and processing data

The analysis methodology uses digital image processing of high resolution of satellite data Landsat 8 for study three typology of impact: heatwaves, drought and wildfire.

The test developed for the heat-waves study uses the following parameters: the Normalized Difference Vegetation Index (NDVI), the Normalized Difference Moisture Index (NDMI) and the Land Surface Temperature (LST). The correlations between NDVI and LST show that the presence of vegetation causes an inversely proportional change in temperature according to a highly significant linear trend, while high NDMI values are understood to represent relatively high vegetation canopy moisture and lower drought stress. The NDMI is the result of the relationship between the difference and the sum of the reflected radiation in the near-infrared and SWIR³.

Droughts and fires are assessed through the study of the Vegetation Health Index (VHI). The VHI index allows to determine the intensity of drought and its spatial extension (Bayasgalan et al., 2006; Bento et al., 2018; Tripathi et al., 2013;). The VHI study shows that the increase land temperatures are assumed to act negatively on vegetation vigor and consequently to cause a stress that favors a fire propensity.

The choice of Landsat-8 images sequences is based on the evaluation of temperatures of the summer months. The selection criteria are as follows: i) year of acquisition; ii) month of acquisition; iii) daily mean temperature; iv) absence of cloud cover⁴.

The selected images (subdivided into geographical area of intervention) are shown below.

³ Short-wave infrared light.

⁴ The selection of the images evaluates the orbital moments of acquisition with a low presence of clouds in the atmosphere.

Municipality	Acquisition-date	Satellite	Name of file	Image quality	T average	T min	T max	Processing result
Udine	20/08 2019	Landsat 8	LC08_L1TP_192028_20190820_20190903_01_T1	good, absence of cloud cover	27°C	20°C	34°C	NDVI, LST, NDMI
Cervia	1/06 2019	Landsat 8	LC08_L1TP_192029_20190601_20190605_01_T1.tar	good, absence of cloud cover	18,5°C	14°C	23°C	NDVI, LST, NDMI
Unione Valle Savio	20/08 2019	Landsat 8	LC08_L1TP_192029_20190820_20190903_01_T1	good, absence of cloud cover	26,5	20°C	33°C	NDVI, LST, VHI
Unione Valle Savio	4/10 2018	Landsat 8	LC08_L1TP_192029_20181004_20181010_01_T1	good, absence of cloud cover	16°C	11°C	21°C	NDVI, LST, VHI
Unione Valle Savio	29/07 2017	Landsat 8	LC08_L1TP_192029_20170729_20170811_01_T1	good, absence of cloud cover	25,5°C	19°C	32°C	NDVI, LST, VHI
Unione Valle Savio	27/08 2016	Landsat 8	LC08_L1TP_192029_20160827_20170321_01_T1	good, absence of cloud cover	23,5°C	17°C	30°C	NDVI, LST, VHI
Unione Valle Savio	8/07 2015	Landsat 8	LC08_L1TP_192029_20150708_20170407_01_T1	good, absence of cloud	31°C	24°C	38°C	NDVI, LST, VHI

				cover				
Vodice	31/08 2019	Lands at 8	LC08_L1TP_189030_20190831_20190916_01_T1	good, absence of cloud cover	27°C	23° C	31° C	NDVI, LST, NDMI
ŠKC	31/08 2019	Lands at 8	LC08_L1TP_189030_20190831_20190916_01_T1	good, absence of cloud cover	27°C	23° C	31° C	NDVI

Table 4 – Selection of the Landsat-8 images

2.2.1.1 Land surface temperature (LST)

The algorithm is implemented in GIS, and it can be used to process the NDVI and LST values. The NDVI parameter allows us to quantify the presence of live vegetation on the ground, while the LST facilitates the understanding of the relationship between temperature and vegetation. This relationship must be considered in relation to the data of cover and land use.

The method uses the Landsat 8 images. The images are available at the Earth Explorer website free of charge. The LST can be calculated according to the following steps.

1. Normalized Difference Vegetation Index (NDVI)

The NDVI index⁵ is calculated according to equation (1), with the reflectances analysis in the near-infrared (RNIR) and red (RRED).

$$NDVI = \frac{R_{NIR} - R_{RED}}{R_{NIR} + R_{RED}} \quad (1)$$

2. Top of Atmospheric Spectral Radiance (TOA)

The second step of the algorithm is the input of Band 10 (10,60÷11,19 µm). The definition of the LST depends on the conversion of the encoding digital numbers (DN) of the band 10 to radiance⁶. The value is computed as follows:

$$L_{\lambda} = M_L Q_{cal} + A_L \quad (2)$$

⁵ The theoretical values are between -1 and +1: normally the presence of vegetation assumes values greater than 0.2, while objects with a value close to or below zero are (generally) anthropic elements.

⁶ Radiance is a variable measured by remote sensing tools. The radiance can be considered as the amount of light that the sensor can capture depending on the observed object. A certain amount of reflected light is dispersed in the atmosphere which absorbs it in part. This decreases the observed brightness and the instrument detects part of the brightness emitted by the object and part of the brightness present in the atmosphere.

where,

L_λ = TOA spectral radiance (Watts/ (m² * sr * μm))

M_L = Band-specific multiplicative rescaling factor from the metadata (0.0003342)

A_L = Band-specific additive rescaling factor from the metadata (0.1)

Q_{cal} = Quantized and calibrated standard product pixel values (DN)

3. Brightness Temperature

After the conversion of the DN to radiance, the thermal Infrared band data should be converted from spectral radiance to brightness temperature (BT)⁷ using the thermal constants provided in the metadata file. This is calculated by the following formula:

$$BT = \frac{K_2}{\ln\left(\frac{K_1}{L_\lambda} + 1\right)} \quad (3)$$

where,

BT = Top of atmosphere brightness temperature (K)

L_λ = TOA spectral radiance (Watts/(m² * srad * μm))

K_1 = Band-specific thermal conversion constant from the metadata (K1_CONSTANT_BAND_774.8853)

K_2 = Band-specific thermal conversion constant from the metadata (K2_CONSTANT_BAND_1321.0789)

4. Proportion of Vegetation

Pv is the proportion of vegetation calculated according to equation (4).

$$PV = \left(\frac{NDVI - NDVI_{min}}{NDVI_{max} - NDVI_{min}}\right)^2 \quad (4)$$

⁷ BT is a parameter that expresses the rate of energy radiated in terms of temperature by a hypothetical black body that emits the same amount of radiation observed.

where $NDVI_{min}$ is the value of $NDVI_{soil}$ and $NDVI_{max}$ is the value of $NDVI_{vegetation}$, extracted from the NDVI image.

5. Land Surface Emissivity

In equation (5), the acronym LSE indicates the value of land surface emissivity. The LSE value must be known in order to estimate LST.

$$LSE = 0.004 * PV + 0.986 \quad (5)$$

6. Land Surface Temperature

The LST raster can be calculated using the central value from the thermal spectral band (w) and the parameter (p), defined according to the Planck constant (6.626×10^{-34} Js, (h)), the Boltzmann constant (1.38×10^{-23} J/K, (S)) and the speed of light (2.998×10^8 m/s, (c)).

$$p = \frac{h * c}{s} \quad (6)$$

$$LST = \frac{BT}{1 + w * \left(\frac{BT}{p}\right) * \ln LSE} \quad (7)$$

where,

BT = brightness temperature

$W = 10.895$

$p = (h * c / \sigma) = 1.438 * 10^{-2}$ mK

LSE = emissivity estimation

For obtaining the results in Celsius, the LST value is revised by adding the absolute zero (8)

$$^{\circ}C = ^{\circ}K - 273,15 \quad (8)$$

The result is a raster map (a key input parameter) for understand the terrestrial thermal behavior.

7. Normalized Difference Moisture Index

This study also evaluates the effect of the NDMI index on urban heat island. NDMI is used to determine vegetation water content the method uses equation (9) taken from the USGS web page for estimate of NDMI.

$$(NIR - SWIR) / (NIR + SWIR) \quad (9)$$

In Landsat 8, NDMI = (Band 5 – Band 6) / (Band 5 + Band 6).

NDMI is used to determine vegetation water content. It is calculated as a ratio between the NIR and SWIR values in traditional fashion. The NDMI defines value from -1 to +1. (+1) indicates a high humidity condition, while (-1) indicates low humidity (or aridity) condition.

2.2.1.2 Vegetation Health Index (VHI)

The VHI index depends on vegetation state and thermal stress, respectively assessed with the Temperature Condition Index (TCI) and the Vegetation Condition Index (VCI). Two indices (TCI and VCI) are calculated, one based on parameters of the Land Surface Temperature (LST) and the other based on parameters of the Normalized Difference Vegetation Index (NDVI).

The VCI index indicates vegetation values that reflect the percentage the soil moisture conditions.

$$VCI = \frac{(NDVI_j - NDVI_{min})}{(NDVI_{max} - NDVI_{min})} * 100 \quad (10)$$

The VCI index indicates vegetation values that reflect the percentage related to vegetative stress related to high temperatures.

$$TCI = \frac{(LST_{max} - LST_j)}{(LST_{max} - LST_{min})} * 100 \quad (11)$$

The VHI index expresses the estimation of the average of the health status of vegetation through a relationship between humidity values and more stressful thermal conditions.

$$VHI = a * VCI + b * TCI \quad (12)$$

where 'a' and 'b' are parameters used to quantify the contribution of each component (TCI and VCI) to the overall vegetation health. ('a' and 'b' define values from 0 to 1). Low VHI values identify areas affected by the drought.

The VHI calculation, in conditions of intense and prolonged extreme events, allows to identify the areas consider drought as a more frequent phenomenon. The concept considers both extreme deficient and surplus rainfall.

The VHI spatialization can help to identify different drought stress gradients which, if properly correlated to specific context information (endogenous and exogenous), can express the potential propensity for a forest to fire.

2.2.2 Using raster DTM for morphodynamic analysis

2.2.2.1 Surface runoff modelling

Using an ad hoc statistical model, it was possible to correlate the run-off coefficients to geomorphological features (DTM) by a variety of land use patterns. Thanks to application of direction and accumulation functions (GIS-based hydrologic modeling), on hydrological impacts (by soil sealing), the model allows to study the dynamic behavior of surface runoff and to quantify the hydraulic impacts related to land use variation.

The study will be accomplished by using the following materials

- DTM 25/5 meters (GeoTIFF format).
- hydrographic reticulum (shapefile format).
- land cover and land use (shapefile format).
- hydrographic basins (shapefile format).

The method converts the general and individual shapefiles in raster format at a pixel of 25 or 5 meters.

The surface runoff index is calculated using the following Equation (13)⁸:

$$\varphi_i = \left\{ \frac{[P \cdot F_U + P^\circ \cdot (F - F_U)]}{F} \right\}_i \quad (13)$$

where,

P= runoff coefficient associated with impermeable areas,

P°= runoff coefficient associated with permeable areas,

F= flow accumulation calculated from the DTM,

F_U= flow accumulation weighted with land use,

U= land use in i.

⁸ See Pozzer, 2015.

The relationship assigns the flow accumulation to the value P. The result is a mapping of the hydraulic impacts ϕ (range from 0,2 to 0,9)⁹. The outcomes show which are the land use most influential on the overall efficiency of the hydraulic system and his regression to less efficient performance. The parameter allows to obtain a correct hydraulic analysis of the catchment and sub-catchment areas to which the settlements belong¹⁰.

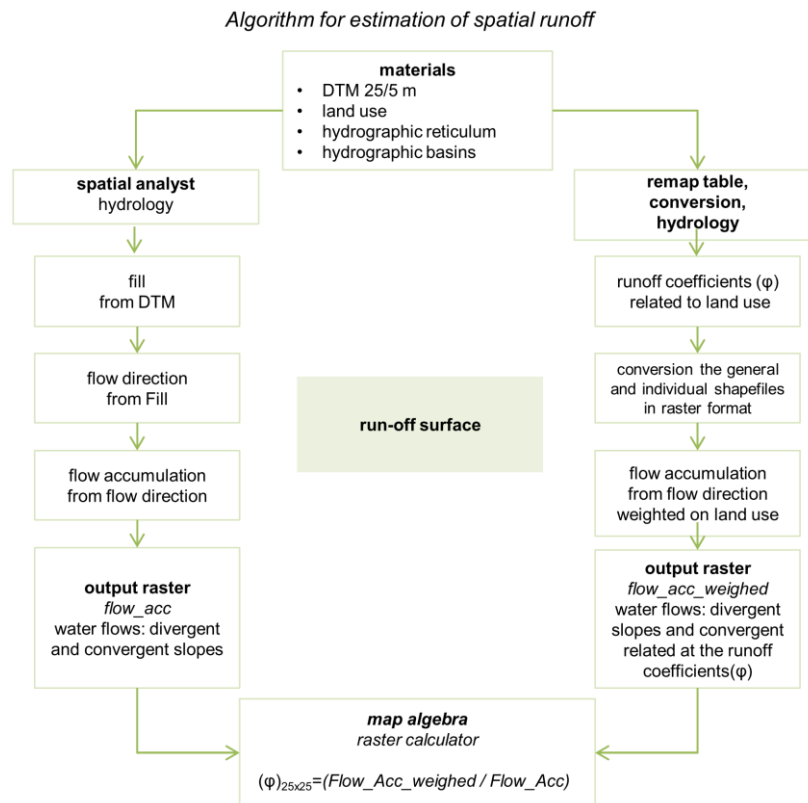


Figure 1 – Flow chart of the algorithm

9 For the choice of runoff coefficients by type of land use, it is recommended to follow the indications of the civil engineering and hydraulic design manuals.

10 The main opportunity for improvement of the survey is as follows: it is necessary to recalibrate these parameters in an acceptance interval based on in-depth analysis also of a geological and climatic nature (climate and microclimate analysis and statistical downscaling models).

2.2.2.2 Areas Susceptible to Coastal Flooding due to SLR

The coastal altimetry is categorized into three classes, by using a method to DTM processing in three scenarios of sea-level rise (compared to the coast): 0.55 meters, 0.75 meters and 1 meter. The processing graphically detects the critical altitude levels of the beach related to a certain probability of occurrence of the phenomenon of rising sea level¹¹.

The elaboration is the following ¹²:

- high probability: $DTM \leq 0,55$ m
- medium probability: $DTM \leq 0,75$ m
- low probability: $DTM \leq 1$ m

¹¹ For information on predicted future increase of sea level for the next 80 years, see [RITMARE project \(www.ritmare.it\)](http://www.ritmare.it) and Marsico et al, 2017.

¹² This analysis is conducted in GIS by using the "raster calculator" function.

2.2.3 Geoprocessing for spatial analysis

The role of geoprocessing tools (overlay analysis, statistical computing, data improvements, and query formation) is to allow the construction of geodatabases capable of optimizing the performance of spatial information. These techniques, combined with zonal statistics functions, allow to maintain a dynamic relationship between the source data and processed data. These processing methods are not activated individually, but are integrated with information from remote sensing analysis activities or related to DTM applications of hydrology or soil analysis. Under this perspective, the information assumes a multi-scalar and multi-disciplinary value. The result is a geographic information system calibrated according to the type of impact and the analysis context.

Geoprocessing/spatial analysis	Impact	Note
<i>Built area fraction</i> : ratio of building plan area to total ground area Overlay between thermal-stress and sensitive-stress, or between thermal-stress and buildings database with the definition of individual functions	<i>Urban Heat Islands</i>	The study supports to define the value of the following variables: sensitivity and adaptive capacity. (for information on <i>sensitivity</i> and <i>adaptive capacity</i> , see following paragraphs)
Landslide mapping: estimation of landslide correlation with the surface runoff raster	<i>Urban flooding/run off/landslides</i>	For the hydrogeological and landslide mapping, see the data sheets relating to the construction of the geographic information of the individual areas of investigation.
Zonal statistics conducted on VHI values; cartographic comparison with wildfire and land use mapping (built and forest)	<i>Wildfire e Drought</i>	The study offers (experimentally test) a contribution to the definition of the potential damage from wildfires
Activation of spatial data analysis functions for the investigation of the plants salt tolerance	<i>Salt intrusion</i>	The procedure will be described in the chapter on the vulnerability assessment of the Municipality of Cervia, section Salt intrusion

Tabella 5 – Attività di geoprocessing e di analisi spaziale di supporto allo studio degli impatti

These activities are fundamental for the evaluation of the following impacts: 'wildfire + drought' e 'salt intrusion'. The calculation procedures of these impacts are described in the next subsections.

2.2.3.1 Geoprocessing applied to assessment of drought and wildfire

Vulnerability is measured in terms of VHI. The processing of Landsat 8 images allows to demonstrate that the increase in temperature has negative effects on conditions of the vegetative state. We note a greater propensity to wildfire for forest and agricultural areas.

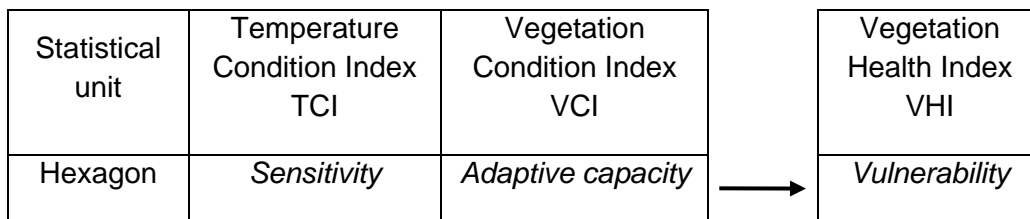


Tabella 5 - Components of the vulnerability

The dynamics of the drought is further analyzed through the estimate of the VHI for 5 different periods: July 2015, August 2016, July 2017, October 2018 and August 2019. This procedure allows to build a large information framework on vegetative stress. The information framework considers the vegetative stresses of the summer and autumn periods. The use of an arithmetic average conducted in GIS between the pixel values of the 5 VHI raster allows to calculate the territorial areas more exposed to drought, and therefore more vulnerable to wildfire.

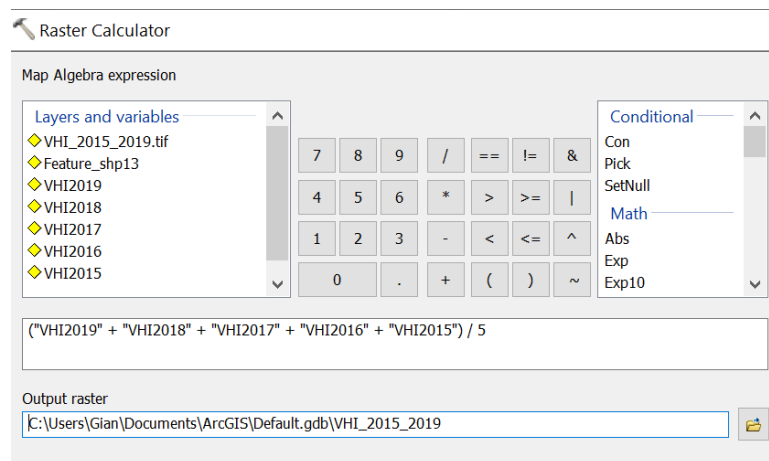


Figure 2 – estimate of the average VHI (2015-2019)

The overlapping of arithmetic result (average value of the VHI 2015-2019) and the wildfire map (2011-2018) shows a certain spatial contiguity between the drought phenomenon and the areas already covered by wildfire.

The second level of processing is conducted to assess the geographical contextualization of the possible damage. The possible damage (D) is here considered a combination of vulnerability and exposure values. The procedure considers the urbanized and forest areas as exposure factors with high wildfire sensitivity¹³. The damage is calculated using the following equation:

$$D = V * E$$

where,

V= vulnerability (VHI)

E= exposure

The cartographic representation of the damage allows to identify the urban areas most exposed to a potential wildfire hazard.

¹³ The uses considered are: residential, industrial, commercial, destinations for public use.

2.2.3.2 Geoprocessing applied to assessment of salt intrusion

The evaluation of the salinity tolerance (and therefore an enhanced propensity to vulnerability) is obtained using two factors: a) salinization class of the soil; b) degree of tolerance of the arboreal species to salinity. The new tolerance thresholds are defined as follows.

<i>Tolerance degree of the arboreal specie</i>	<i>Soil salinity</i>		<i>Degree of tolerance: new assignment</i>		<i>Propensity to vulnerability</i>	<i>Value point statistics</i>
	Very saline	<input type="checkbox"/>	Unvaried	<input type="checkbox"/>	Not significant	1
High <input type="checkbox"/>	Weakly saline	<input type="checkbox"/>	Unvaried	<input type="checkbox"/>	Not significant	1
	Not saline	<input type="checkbox"/>	Unvaried	<input type="checkbox"/>	Not significant	1
<i>Tolerance degree of the arboreal specie</i>	<i>Soil salinity</i>		<i>Degree of tolerance: new assignment</i>		<i>Propensity to vulnerability</i>	<i>Value point statistics</i>
	Very saline	<input type="checkbox"/>	Medium low	<input type="checkbox"/>	Moderately significant	2
Medium <input type="checkbox"/>	Weakly saline	<input type="checkbox"/>	Low	<input type="checkbox"/>	Not significant	1
	Not saline	<input type="checkbox"/>	low	<input type="checkbox"/>	Not significant	1
<i>Tolerance degree of the arboreal specie</i>	<i>Soil salinity</i>		<i>Degree of tolerance: new assignment</i>		<i>Propensity to vulnerability</i>	<i>Value point statistics</i>
	Very saline	<input type="checkbox"/>	Low	<input type="checkbox"/>	Significant	3
Low <input type="checkbox"/>	Weakly saline	<input type="checkbox"/>	Low	<input type="checkbox"/>	Moderately significant	2
	Not saline	<input type="checkbox"/>	Unvaried	<input type="checkbox"/>	Not significant	1

Table 6 – Vulnerability assessment of arboreal species

This methodology allows to define a first spatial vulnerability of arboreal species. The effect can be traced back to the phenomenon of 'salt intrusion'. The processing identified three classes:

- Not significant.
- Moderately significant.
- Significant.

Each entity class is associated with a value from 1 to 3: not significant = 1; moderately significant = 2; significant=3.

2.3 Geodatabase

The information derived from remote sensing analysis and the contents elaborated by geoprocessing activities have been aggregated into two different types of databases:

1. The results of the analysis of remote sensing data were aggregated into 'orchestrator geodatabases'. These geodatabases are designed concerning the characteristics of the study area and the impact typology
2. The raster and vector information bases have been archived by subject area and crossed and spatially evaluated in the GIS environment.

The first type of database needs further comment regarding the collecting and organizing method of information. The database is organized in a single table projected on a hexagonal matrix. Each hexagon (statistical unit) has a side of 80 (or 30) meters. Each statistical unit corresponds to a row of the table. Each row is related to a set of variables. The variables correspond to the information and all the indicators for each hexagon. The indicators are represented on a values scale defined from 0 to 1¹⁴. The hexagon database supports a methodology analysis that combines high-resolution spatial information and geospatial data to develop sensitivity, adaptive capacity and vulnerability. Vulnerability is considered a synthetic index obtained as the difference between the sensitivity and adaptive capacity parameters.

The impacts with a hexagonal matrix are as follows: UHI, runoff, Wildfire e Drought.

¹⁴ This operation allows to aggregate values endowed of a non-comparable rank of variability.

2.4 Vulnerability assessment methodologies: definition of assessment indicators

At the end of the data-processing operation, the work is expected to quantify the heterogeneity and spatial distribution of impacts through two types of surveys:

- study of non-linear variables, not punctual and external to the properties of the environment (surveys through satellite image processing; references on climate variability and change);
- study of linear variables such as morphological elements and ecosystem frameworks, natural and artificial. These elements help to define a degree of vulnerability that varies according to their size and their coexistence in each part of the territory.

The general methodology (Fig. 3) provides a model of territorial analysis for the governance and urban planning. This model is based on tools that can recognize different levels of the dynamics of impact:

- a) variations in climate impact (in terms of UHI¹⁵);
- b) building and natural environment morphologies;
- c) human infrastructure;
- d) characteristics and quality of ecosystems.

¹⁵ See Oke (1982).

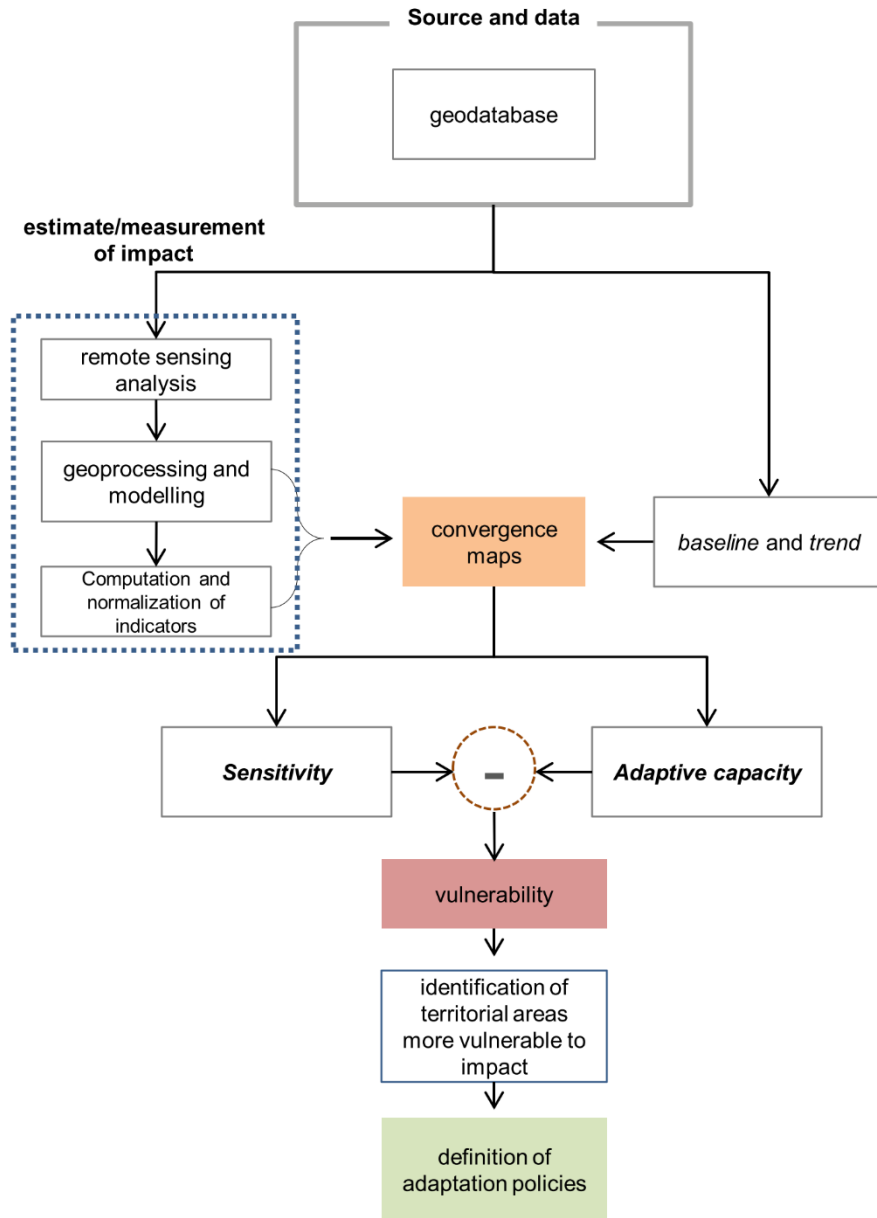


Figure3 – Flow chart for the morphological study of impacts

The assessment of the vulnerability of an urban environment (or natural system) requires adequate knowledge of the morphological structure of the city, its materials, an appropriate reading on the variation of environmental complexity and its ecosystem services. To study the vulnerability of a territory, the reference scientific literature considers four analysis variables: sensitivity, exposure, adaptive capacity, potential impact¹⁶. This work uses only two indicators, the sensitivity and adaptive capacity¹⁷. Their adoption makes the vulnerability study replicable both on an urban and territorial scale (city or territory), based on the following expression:

$$V = \text{sensitivity} - \text{adaptivecapacity} \quad (14)$$

where,

sensitivity = “propensity of a system to be impacted”.

adaptive capacity = “propensity of a system to mitigate impact”.

The measurement of sensitivity and adaptive capacity indicators is influenced by three main factors:

- land exposure and sensitivity to climate change;
- limited number of map information levels;
- degree of potential of GIS surveys in recognising new spatial correlations between territorial elements that maximise the impact on the environment, returning typological variations that can mitigate the impact.

¹⁶ See Maragno (2018).

¹⁷ The reason for considering only sensitivity and adaptive capacity is dictated by precise methodological choices already tested in the field of analysis of the 'new vulnerabilities', explained for different combinations of environmental variables (Maragno, 2018). Sensitivity, "in the IPCC approach, determines the degree to which a system is adversely affected by a given exposure" (see Maragno, 2018: 30). It depends on the specific properties of the system under consideration. Adaptive capacity can be considered as that ability by a natural or built system to adapt to climate change, in order to moderate potential impacts and/or damage. In Maragno (2018) it is considered as a set of drivers for the choice of compensatory measures.

These factors affect the content of the indicators and their interaction in the evaluation process.

Equation (14) is reviewed and weighted according to different analysis and research possibilities. The calibration varies based at the information typologies and the methods for estimating the sensitivity and adaptive capacity variables. To develop a plausible estimate of all impacts, equation (14) is redesigned in a GIS environment based on the characteristics of the impact and the context conditions (table 8).

Impact	Statistical unit	Source and data	Vulnerability		Estimate of vulnerability
			Sensitivity	Adaptive capacity	
Urban Heat Islands	hexagon (side of 80 m)	<ul style="list-style-type: none"> land surface temperature (LST) normalized difference vegetation Index (NDVI) normalized difference water index (NDMI) building surface 	<ul style="list-style-type: none"> LST (average value) building densities 	<ul style="list-style-type: none"> NDVI (average value) NDMI (average value) 	<p>$V = \text{sensitivity} - \text{adaptive capacity}$</p> <p>The vulnerability lies in a range of values between -1 and 1. Negative values correspond to good adaptive performances, while positive values correspond to critical conditions.</p> <p>In this study the vulnerability is normalized from 0 to 2, where low values correspond to critical conditions, while positive values correspond to good adaptive performances.</p>
Urban flooding	Pixel; hexagon (side of 80 m)	<ul style="list-style-type: none"> DTM land use runoff coefficients 	0,9 soil sealing	0,1 permeable areas	<p>The equation '$V = S - A$' is processed with a Gis using the Hydrology function. The Hydrology function allows to calculate a behavior raster relating to the hydraulic system of the area.</p> <p>The equation allows you to assign the runoff coefficients to the flow accumulation (Flow_Acc). This procedure generates the 'hydraulic impacts' ϕ (raster cell). This correlation is expressed as a percentage of rain that turns into surface runoff (with a range from 0.1 to 0.9). The procedure,</p>

					calibrated at the basin scale, is cumulative..
Wildfire Drought	Pixel; hexagon (side of 30 m)	Vegetation Index (VHI) Health	temperature condition index TCI	vegetation condition index VCI	The relationship 'V = S-A' is measured as VHI. The study proposes to consider the forest and the built environment as factors maximizing the drought phenomenon. Builds and forests are here considered as elements of exposure. The use of these elements supports the construction of a map of the wildfire potential damage for natural or man-made environments.
Landslides	The landslide phenomenon is mapped and studied in associations with the study of urban flooding (runoff calculated to basin-scale)				
Sea-level rise	The sea-level rise is studied through the evaluation of the relative rise in sea-level in the coastal areas. The method processes a DTM with a cell of 5x5, then comparing it with the information contained in the map of hydraulic and coastal criticalities.				
Salt intrusion	tree	<ul style="list-style-type: none"> • degree of soil salinity • degree of tolerance to salinity 	degree of soil salinity	degree of tolerance to salinity	The equation 'V = S-A' is processed with a Gis with geoprocessing functions. These functions allow to calculate a vector of qualitative-qualitative behavior of resistance of the arboreal species in the presence of saline contents of the subsoil.

Table 7 – Methodologies to support vulnerability assessments

3 Conclusions

This study-activity has developed a methodology for resilient representation of the territory and to provide local communities with efficient and effective climate change adaptation planning models. These models can ensure an adequate level of economic and social well-being for the local urban environment. The study has analyzed some impact potentially adverse to the dynamics of vulnerability of the pilot adriatic territories. The results are presented in the deliverables *D.5.1.2. Vulnerability and feasibility analysis for each pilot area*.

4 Glossary

CMCC: Centro euro-Mediterraneo sui Cambiamenti Climatici

DTM: Digital Terrain Model

LST: Land surface temperature

LSE: Land surface emissivity

VHI: Vegetation Health Index

NDVI: Normalized Difference Vegetation Index

NDMI: Normalized Difference Moisture Index

SWIL: Short-wave Infrared Light

BT: Brightness Temperature

TOA: Top of Atmospheric Spectral Radiance

TCI: Temperature Condition Index

VCI: Vegetation Condition Index

5 References

- Arnbjerg-Nielsen K., Willems P., Olsson J., Beecham S., Pathirana A., Bülow Gregersen I., Nguyen V. T. V. (2013), "Impacts of climate change on rainfall extremes and urban drainage systems: a review", *Water Science and Technology*, 68(1), 16-28.
- Autorità di bacino del fiume Po (Adbpo) (2006), *Caratteristiche del bacino del fiume Po e primo esame delle attività umane sulle risorse idriche*, Parma.
- Bayasgalan M., Bayarjargal Y., Agam N., Khudulmur S., Tucker C.J., (2006), "Comments on the use of the vegetation health index over Mongolia", *Int. J. Remote Sens.*, 27, 2017–2024.
- Bento V.A., Trigo I.F., Gouveia C.M., DaCamara C.C., (2018), "Contribution of land surface temperature (TCL) to vegetation health index: A comparative study using clear sky and all-weather climate data records", *Remote Sens*, 10, 1324.
- CMCC (2017), *Piano Nazionale di Adattamento ai Cambiamenti Climatici – PNACC. Allegato tecnico-scientifico impatti, vulnerabilità e azioni di adattamento settoriali*, Venezia (versione luglio 2017).
- Comune di Cervia – Settore Programmazione e Gestione del Territorio (2016), *Relazione geologica Fascia costiera*.
- Girardi S. (2014), "Cuneo salino: fattore limitante per il delta del Po", *Agriregionieuropa*, 10(37), disponibile su: <https://agrireregionieuropa.univpm.it/it/content/article/31/37/cuneo-salino-fattore-limitante-il-delta-del-po>
- IPCC (2014), *Climate Change: Impacts, Adaptation, and Vulnerability*, Cambridge University Press, Cambridge.
- Maas E. V. (1986), "Salt tolerance of plants", *Applied Agricultural Research*, 1(1), pp. 12-26.
- Maas E. V. (1996), "Plant response to salinity". 4th National Conference and workshop on the Productive Use and Rehabilitation of Saline Lands, Published by Promaco Conventions PTY LTD, Albany Western Australia.
- Maragno, D. (2018), *Ict, resilienza e pianificazione urbanistica. Per adattare la città al clima*, Milano: Franco Angeli.
- Margeta J. et al., (2016). Integrated Coastal management Plan of Šibenik-knin county, in *PAP/RAC u suradnji s razvojnim agencijama: "Prema održivom razvoju obale"*.
- Marsico A., et al. (2017), "Flooding scenario for four Italian coastal plains using three relative sea level rise models", *Journal of Maps*, 13(2), 961-967.

- Munns R. (1999), "The impact of salinity stress", The Foundation for Sustainable Agriculture – Coping with Plant Environment Stress.
- Oke T.R. (1982), "The energetic basis of the urban heat island", *Quarterly Journal of the Royal Meteorological Society*, 108(455), 1-24.
- Oude Essink G. H. P. (2001), Improving fresh groundwater supply – problems and solutions, *Elsevier, Ocean & coastal management* 44, pp.429-449
- Pileri P. (2007), *Compensazione ecologica preventiva. Principi, strumenti e casi*, Roma: Carocci Editore.
- Pileri P. (2015), *Che cosa c'è sotto. Il suolo, i suoi segreti, le ragioni per difenderlo*, Milano: Altreconomia Edizioni.
- Pozzer G. (2015), "Consumo di suolo e gestione del rischio idraulico: test per l'invarianza idraulica nella pianificazione territoriale", in Munafò M., Marchetti M., a cura di, *Recuperiamo terreno. Analisi e prospettive per la gestione sostenibile della risorsa suolo*, Milano: Franco Angeli, pp. 168-180, ISBN 9788891713858.
- Regione Emilia-Romagna, Servizio Geologico, Sismico e dei Suoli (2011), *Carta della salinità dei suoli della Pianura emiliano-romagnola. Strato 50-100 cm*. Prima approssimazione scala 1:250.000.
- Savenije H. H. G. (2005), *Salinity and tides in alluvial estuaries*, Delft University of Technology, Elsevier, Delft, The Netherlands.
- Shannon M. (1997), "Adaptation of plants to salinity", *Advances of Agronomy*, 60, pp. 5-120.
- Šibenik Knin County (2016), *Coastal Plan of the Šibenik Knin County*.
- Lerer S. M., Arnbjerg-Nielsen K., & Mikkelsen P. S. (2015), "A mapping of tools for informing water sensitive urban design planning decisions-questions, aspects and context sensitivity", *Water*, 7(3), 993-1012.
- Tosi L., Di Sipio E., Carbognin L., Zuppi G. M., Galgaro, A. Teatini P., Bassan V., Vitturi A. (2011), "Intrusione Salina", *Atlante Geologico della Provincia di Venezia. Note Illustrative*, Provincia di Venezia.
- Tripathi R., Sahoo R. N., Gupta V. K., Sehgal V. K., Sahoo P. M., (2013), "Developing vegetation health index from biophysical variables derived using MODIS satellite data", in the *Trans Gangetic plains of India*, *Emirates J. Food Agric*, 2013, 25(5), 376–384.